SEA vehicle model for rolling- and engine noise

F. Nentwich[1], T. Bartosch[1], G. Müller[1]

[1] MAGNA STEYR Fahrzeugtechnik, A-8041 Graz, Austria, Email: fred.nentwich@magnasteyr.com

Introduction

A predictive Auto-SEA model is set up for a front driven car, as shown in fig.1. It deals with coast down rolling noise [12] and runup engine noise. The body's geometry in SEA is based on a FEM model. The trim's acoustic behaviour is either measured or estimated with Auto-SEA. The excitation is measured on a forerunner vehicle. Together, structure and excitation provide a simulation valid at mid and high frequencies, i.e. 400 Hz - 6.3 kHz.

SEA balances the power fed into the system with internal power flows and dissipation [5]. The original excitations are virtually replaced by the power inputs P_b and energy levels E_b of the model's adjoining subsystems [4] [10]. These levels are measured on a forerunner and are subsequently imposed on the subsystems as boundary condition. Subsequently two types of subsystems are distinguished: normal subsystems "s" with no external power input and an unknown energy $\underline{E_s}$, and boundary condition subsystems "b" with the input power $\underline{P_b}$ und a preset energy $\underline{E_b}$. The system matrix $\mathbf{L}$ is composed of $\mathbf{L_{bs}}$, $\mathbf{L_{bs}}$, $\mathbf{L_{ss}}$ and $\mathbf{L_{bb}}$. The last two matrices are square. The system matrix contains the subsystems' coupling loss factors and internal loss factors, which describe the interchange of the subsystems' energies and dissipation.

$$\omega \underbrace{\begin{bmatrix} \mathbf{L_{ss}} & \mathbf{L_{sb}} \\ \mathbf{L_{bs}} & \mathbf{L_{bb}} \end{bmatrix}}_{\{M_s+M_b\}\times\{M_s+M_b\}}, \underbrace{\begin{bmatrix} \underline{E_s} \\ \underline{E_b} \end{bmatrix}}_{\{M_s+M_b\}\times\{1\}} = \begin{bmatrix} \underline{0} \\ \underline{P_b} \end{bmatrix}, \text{ [W]} \quad (1)$$

Application

The Auto-SEA model describes a front driven car with a 140 kW engine. The structure stems from the FEM model of a vehicle yet to be built. The excitation was measured on an existing forerunner model, whose gasoline engine had 150 kW instead of 140 kW, at the roller dynamometer. The model comprises 957 subsystems of which 3 × 292 are plates capable of extension waves, shear waves and flexure waves, 19 interior cavities and 62 exterior cavities. The matrix L has 25.400 non-zero elements and a sparcity of 4%. Excluding the reciprocal CLFs that leaves 12.900 CLFs and ILFs together per frequency. This formulation enables a simulation of how trim variations impact the car's acoustics.

Structure

The metal sheet's geometry and thickness are based on the latest FEM model available at the start of the SEA calculations. The power train and the chassis are not part of the model. Stiffening corrugations, small leakages and minor gaps are not modelled.

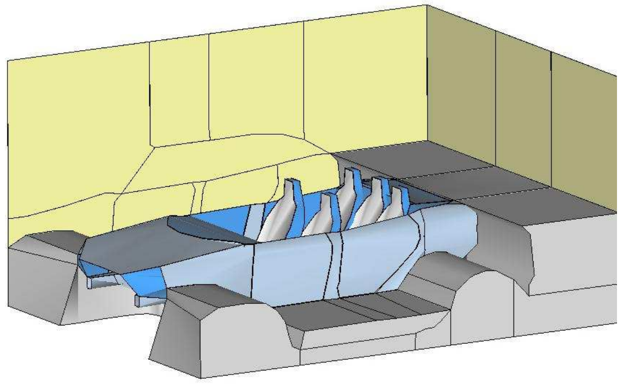

Figure 1: Geometric SEA Model. The steel structure (steel blue) is fitted with plastic interior (blue) and leather seats (white). The car is embedded in exterior air volumina (grey) which are confined in a box of 100%-absorbers (yellow). The greenhouse has been removed for visibility.

SEA's validity is bound to a high modal density which is provided at high frequencies and for large subsystems. On the contrary, rolling and engine noise are dominated by low and mid frequencies. To cover them more efficiently it is suitable to focus on expanding the validity's lower edge frequency downward [4]. The simplest is to promote large subsystems by alloting special attention to the junction of hollow profiles, beam like structures and anti drumming pads. **1.** In Auto-SEA, plate subsystems can be connected at their edges, but not on their surfaces. This software characteristic influences the subsystems' definition, arrangement and boundaries. In the case of a junction of several hollow profiles, for the sake of subsystem connection, the engineer is prompted to subdivide the junction into several subsystems even though he would judge the junction structure as one subsystem in terms of energy level. This would artificially lower the modal density. Thus special care is taken for defining the subsystems. **2.** Several closely spaced parallel steel strips at times constitute a beam like structure composed of plates. This "beam structure" often has variable bending stiffness tailored to optimally suit its stress while minimizing weight. In the SEA model, these strips are merged to one subsystem. Its thickness has the equivalent total bending stiffness as the strip ensemble. **3.** Here, anti drumming pads are modelled as laminates. An anti drumming pad often covers only a fraction of its plate. Instead of splitting up the plate into several subsystems, the anti drumming pad is uniformly spread across the plate keeping their total mass constant [7, p.49]. Thus only one subsystem is necessary. An alternative is, to model the partial anti drumming pads as multiple noise controll treatments.

The trim data is derived from analytical models or acoustic measurements. Analytical models are employed for carpets, head liner, door liner and panelling. They use geometry and material information to calculate the absorption index and transmission loss. Their input data is subject to some uncertainty: on the construction drawing, the thicknesses of a composite material may vary across the panel. Further, the component's material's name ("polyurethane foam") provided by the construction drawing often indicates a whole class of derivatives. Their acoustic properties strongly depend on chemical composition and processing and sometimes have a wide range. These foam parameters have either been measured by professional suppliers or are estimated values. To complement this, the absorption index and transmission loss factor were measured on either on the original material itself or on a similar material of a preceding project. The latter was done for the leather seats, the engine bay's damping and for the equivalent volume of the wheel house.

Excitation

The excitation applied to the SEA model is obtained from forerunner vehicle measurements. The actual excitation, like the engine's combustion, is too costy and time consuming to measure. Instead the subsystems, where the excitation is induced into the car body [10], are regarded as vibration sources of the SEA model. The vibrations of these source subsystems are measured at multiple points, averaged both spatially and temporally and subsequently defined as boundary conditions. Analogously, the air space surrounding an air-borne excitation source (tyre road contact) is regarded as the SEA model's sound source. Here, the sound pressure is measured, averaged and imposed as boundary condition in the SEA model. Using the concept of equivalent mass m_{eq} and volume V_{eq} [6] the energies of both air and structure-borne source subsystem are defined.

$$E_{(b)} := \begin{cases} m_{eq}\, \bar{v}^2_{(b)} & \ldots \text{structure-borne} \\ \dfrac{V_{eq}}{cZ_o}\, \bar{p}^2_{(b)} & \ldots \text{air-borne} \end{cases} \qquad [\text{J}] \quad (2)$$

The $E_{(b)}$ is applied as a constraint to (1). The corresponding input sound power $P_{(b)}$ however is unknown. It is formally exchanged for a virtual energy by using the element wise substitution $E_{(p)} := P_{(b)}/\omega$. The virtual energies are collected in $\underline{E_p}$. The matrix $\mathbf{I}$ measures $M_b \times M_b$ and has ones in the diagonal.

$$\omega \underbrace{\begin{bmatrix} \mathbf{L_{ss}} & \mathbf{L_{sb}} & \mathbf{O} \\ \mathbf{L_{bs}} & \mathbf{L_{bb}} & -\mathbf{I} \end{bmatrix}}_{\{M_s+M_b\}\times\{M_s+M_b+M_b\}} \underbrace{\begin{bmatrix} \underline{E_s} \\ \underline{E_b} \\ \underline{E_p} \end{bmatrix}}_{\{M_s+M_b+M_b\}\times\{1\}} = \underbrace{\begin{bmatrix} \underline{0} \\ \underline{0} \end{bmatrix}}_{[\text{J}]} \quad (3)$$

The constrained energy $\underline{E_b}$ is rearranged to the right side of the equation making it suitable for solution.

$$\omega \begin{bmatrix} \mathbf{L_{ss}} & \mathbf{O} \\ \mathbf{L_{bs}} & -\mathbf{I} \end{bmatrix} \begin{bmatrix} \underline{E_s} \\ \underline{E_p} \end{bmatrix} = \underline{P_{mod}}, \qquad [\text{W}] \quad (4)$$

The source system's velocities $\bar{v}$ and sound pressures $\bar{p}$ were measured on the forerunner vehicle on the roller dynamometer. The roller dynamometer may possibly contribute to some dynamometer noise and barrel repetition orders. Measures are taken to minimize these artefacts [8] [9]. For the engine noise the load cases: wide open throttle run-up, open throttle run-up, stand still run-up and idling are measured. For the rolling noise the load cases: turning front wheels, turning back wheels and all wheels turning are measured. The structure-borne excitation subsystems are: the front axle carrier, the rear axle carrier, 2 engine carriers, 2 rear longitudinal members and 4 strut towers. The air-borne excitation subsystems are: the engine bay, 4 wheelhouses and 4 underfloor cavities. The forerunner vehicle by and large represents the newly developed vehicle simulated although the rear axle carrier has been modified. Assuming that the source velocities of forerunner vehicle and newly developed vehicle are identical, the measured excitations are directly applied to the SEA model.

Separating the rolling and engine excitation is difficult. When measuring the rolling noise the engine is presumably turned off with the gear on neutral. If this is not possible (automatic four wheel drive) the gear is put on neutral and the engine is left idling thus contributing some engine noise to the rolling noise measurement. Vice versa, when the engine noise is measured, the engine's power must be led somewhere. On the dynamometer rig the wheels do the job – and additionally cause rolling excitation. For consistency of model and validation it is crucial to measure all excited subsystems. Measurements targeting the engine noise sources therefore also include the rolling noise sources and vice versa.

Exterior Sound Field

The exterior sound field is roughly modelled as a semi anechoic chamber: walls and ceiling have an absorption index of one, and the floor is reverberant. The anechoic chamber's air space is filled with 51 exterior cavities. The cavities underneath the car and in the wheel houses are regarded as sound sources. The directional sound field surrounding the car is approximated by a set of diffuse sound fields. This underemphasizes the waves travelling away from the vehicle and overemphasizes the waves returning to the vehicle. Nevertheless the perimetric energy interchange of the outside field and its energy loss into the far field are by and large taken into account realistically. The exterior sound field has a minor influence on the interior sound only. Thus this propagation model is sufficient.

Plausiblisation

For the measurement, only a similar forerunner vehicle was available. Thus no validation is possible. Instead, forerunner measurement and simulation are compared in a plausiblisation. Differences occurring may stem from modelling errors, measurement errors, prototype scatter or differences in design between actual vehicle and forerunner vehicle. The maximum difference of simulation and measurement in 400 Hz–6.3 kHz band-pass sound pressure level (BPSPL) is 2 dB(A) for engine noise (fig.2) and 3 dB(A) for the rolling noise (fig.3). Regarding the $1/3^{rd}$ octave band levels of the engine noise (fig.4) most of the simulation (97%) lies within a ±5 dB-band of the measurement. For the rolling noise (fig.5) there is a deviation spot of 10 dB(A) difference at 630 Hz and 40–50 km/h. Nevertheless most (89%) of the rolling noise simulation's $1/3^{rd}$ octave band levels still lie in the ±5 dB-band of the measurement.

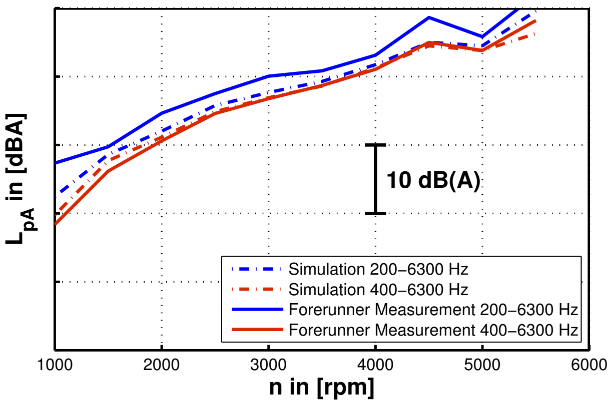

Figure 2: Engine Noise Plausibilisation: 400–6300 Hz BPSPL(A) as function of rotational speed at wide open throttle on roller dyno. Maximum difference: 2 dB(A).

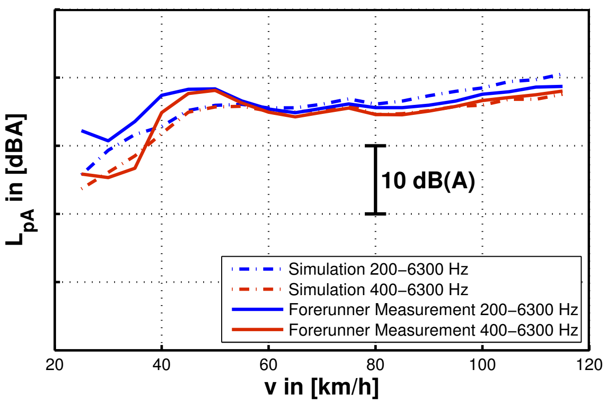

Figure 3: Rolling Noise Plausibilisation: 400–6300 Hz BPSPL(A) as function of speed on roller dynamometer with only the front wheels turning. Maximum difference: 3 dB(A).

Trim Package Optimization

A 12 kg-trim package targeting the noise transmission has been designed beforehand. It can be added at a late stage, if necessary. The trim package consists of heavy layers on floor, fire wall and trunk and cotton vlies in the

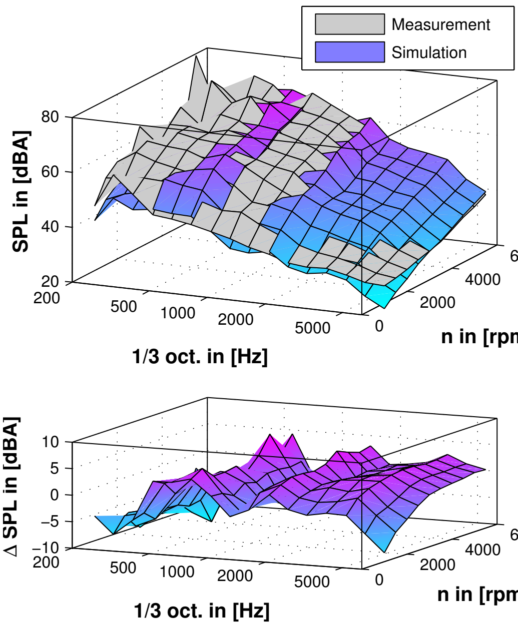

Figure 4: Engine Noise Plausibilisation: $1/3^{rd}$ octave band SPL at wide open throttle on roller dynamometer as function of rotational speed and frequency. Above: simulation and forerunner measurement. Below: SPL difference.

fender cavites and in the trunk. Since additional weight increases fuel consumption the question is, which parts of this trim package are most effective? The vibro-acoustic potential analysis of car with no extra trim yields the most sensitive CLFs and ILFs. It reveals that the heavy layer on the fire wall and the front part of the floor are particularly effective. These identified *parts* of 12 kg-trim are reassembled to a new trim subset weighing 4 kg. The upper pannel of fig.6 shows, that in comparison to the vehicle without extra trim, up to 3 dB(A) improvement in BPSPL are achieved by installing the 4 kg-trim subset. The pannel below shows, that difference between the 4 kg-trim and 12 kg-trim is smaller than $\frac{1}{10}$dB(A), i.e. insubstantial. In other words, the *not* chosen 8 kg have no or little effect on the interior noise. With help of the VAPA, the 4 kg-trim targeting the dominant transfer path was derived. The importance of identifying the dominant transfer path and its sensitivity to component measures is also underlined by other methods like the transfer path analysis [9] [11]. Impressively, the 4 kg-trim subset, which was identified with the VAPA, has the same effect on rolling noise and engine noise as the original 12 kg-trim even though it weighs only a third.

Synopsis

A SEA-Simulation at 400 Hz–6.3 kHz is conducted for engine and rolling noise of a front driven car. The plausibilisation on a forerunner reveals an accuracy of ±3 dB(A) in BPSPL and ±5 dB(A) in most (≥ 89%) of the $1/3^{rd}$ octave band levels. A single constructional measure often results in a small relative change. Due to measurement scatter, this change is difficult to detect experimentally. The SEA-model can resolve these fine relative changes. The model can help judge and optimize

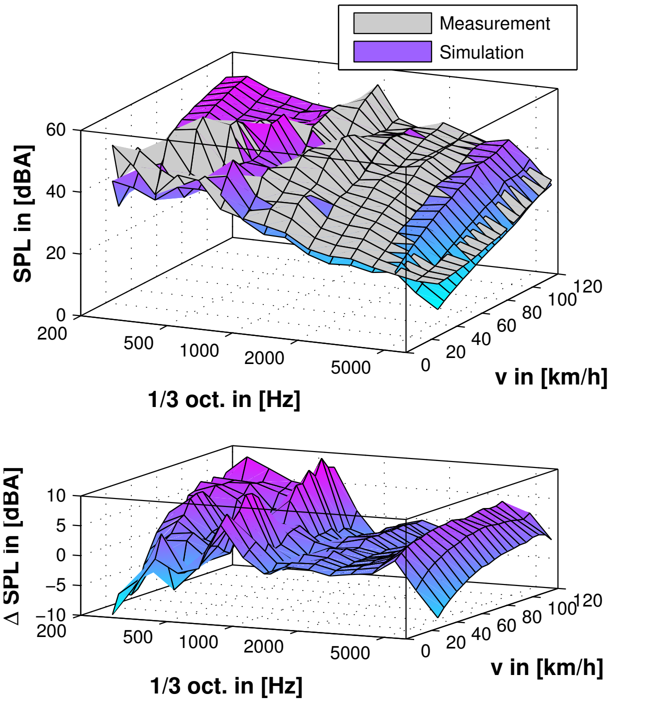

Figure 5: Rolling Noise Plausibilisation: $1/3^{rd}$ octave band SPL as function of speed and frequency on the roller dyno with only the front wheels turning. Above: simulation & forerunner measurement. Below: SPL difference.

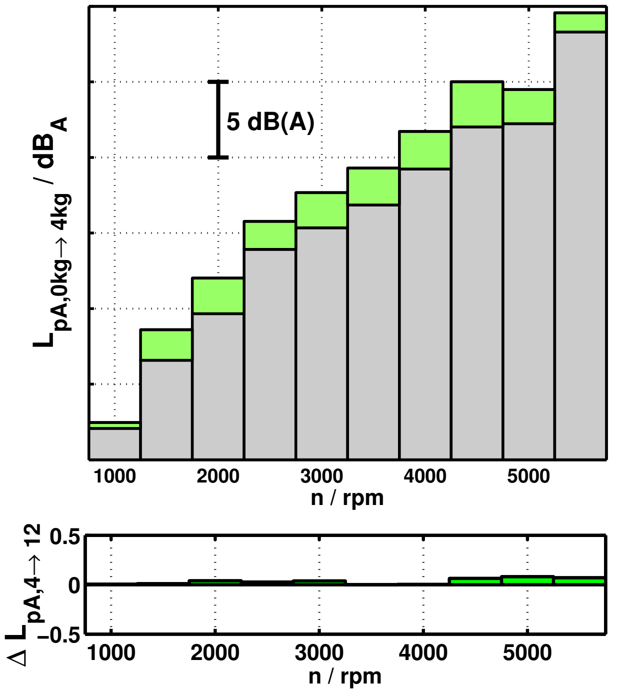

Figure 6: Optimization of Engine Noise: 400–6300 Hz BPSPL(A) as function of rotational speed at wide open throttle on the roller dynamometer. Above: The green areas show the improvement of the 4 kg-trim package. Below: In comparison to the 4 kg-trim package the 12 kg-trim package yields only $1/10^{th}$dB(A) improvement. This proves the effectivity of the 4 kg-trim package.

constructive measures. From an original package the most effective components were identified. Impressively, the lighter 4 kg-trim package yields the same engine noise reduction as the 12 kg-trim package.

References

[1] T. Bartosch, H. Macher, B. Kastreuz, C. Fankhauser: Optimize the acoustic concept using SEA vibro-acoustic potential analysis. In: *NVH Excellence - Achieving Results beyond Customer Expectations*, p. 133-143, Graz, Austria, 15-17 Nov. 2006. ACC, AVL, MAGNA STEYR and SAE International.

[2] T. Bartosch, T. Eggner: Engine noise potential analysis for a trimed vehicle body: Optimisation using an analytical sea gradient computation technique. *JSV* **300** (1-2), 1-12, Feb. 2007.

[3] T. Bartosch, G. Müller, T. Eggner: Vibro-acoustic optimisation process based on hybrid SEA modelling of a trimed body vehicle. *Proc. of Joint Meeting of the German and the French Acoustical Societies, Fortschritte der Akustik,* Stuttgart, Germany, 19-22. Mar. 2007. DEGA, Univ. Stuttgart, Fraunhofer IBP.

[4] T. Bartosch, T. Eggner, K. Kolrus, H. Zach, G. Müller: Simulationsgesttzte Optimierung des Rollgeräusches im mittel- und hochfrequenten Bereich mit der Vibroakustischen Potenzialanalyse. *In: SIMVEC 2008, VDI-Berichte* **2031**, Baden-Baden, Germany, November 2008. VDI.

[5] R. DeJong, R. H. Lyon: *Theory and Application of Statistical Energy Analysis*, Verl.: Butterworth-Heinemann, Newton/USA 1995.

[6] P. Gelat and N. Lalor: The role and experimental determination of equivalent mass in complex SEA models. *JSV* **255** (1), 97-110, 2002.

[7] S. Korte: *Untersuchung der hochfrequenten akustischen Tranmission einer Kfz-Bodengruppe mittels Statistischer Energieanalyse.* TU Berlin, Diss., 2005.

[8] W. Kropp: Reifen-Fahrbahn-Geräusch, Modellieren als ein Weg zum Verständnis, In: *Fortschr. d. Akustik, DAGA 2005*, (DEGA Berlin, CD-ROM, 2005).

[9] F. Nentwich, H. Finsterhölzl, H. Fastl: Darstellung und Beurteilung von Rollgeraeusch-Anteilen, *Fortschr. d. Akustik, DAGA 2002*, 208–209 (2002).

[10] F. Nentwich: *Transfer-Pfad-Analyse im Zeitbereich zur Auralisierung von PKW-Innengeräuschen,* Shaker, Aachen, 2004.

[11] F. Nentwich, Presentation of the Transfer Path Analysis of the Car's Interior Sound via Headphones, In: *Proc. of the 13^{th} International Congress on Sound and Vibration* (ICSV13), Vienna, Austria, 2006.

[12] G. Müller, T. Bartosch, and T. Eggner. Optimisation of tyre noise transmission of a compact class vehicle using an experimental sea model. In *Proc. of EuroPAM user conference,* Toulouse, Frace, 10-12 October 2006. ESI Group.